

*Invited Paper***Terahertz isolator based on magneto-microstructure**

Sai. Chen, Fei. Fan, and Sheng-Jiang. Chang *

Institute of Modern Optics, Nankai University, Tianjin 300071, China

* Email: sjchang@nankai.edu.cn

(Received August 18, 2015)

Abstract: In this paper, we have reviewed our study in terahertz (THz) isolators and nonreciprocal transmission devices, with an emphasis on novel isolators based on a new kind of physical mechanism. In combination with microstructure and magneto-optical material, we have presented different forms of THz isolators, such as plasmonic waveguides, plasmonic lens, photonic crystal cavity and magneto-metasurface. Moreover, we have discussed and concluded the necessary conditions of forming THz nonreciprocal transmission in the magneto-microstructure devices, which is strongly related with magneto-material and asymmetric transmission system. THz isolators are important for the realization high efficient THz systems.

Keywords: Terahertz spectroscopy, Isolators.

doi: [10.11906/TST.145-156.2015.12.14](https://doi.org/10.11906/TST.145-156.2015.12.14)

1. Introduction

With great successful progress on terahertz (THz) science and technology [1-6], more and more applications in imaging, sensing and communication have been realized [7-9]. For further development of the THz application system, there is a high demand on efficient devices, such as waveguide [10], switch [11-14], modulator [15-23], filter [10, 24-26], polarizer [27-30], lens [8, 31, 32] and isolator [33-39] for guiding, transmitting, modulating, controlling and manipulating THz waves. In order to be efficient, novel artificial electromagnetic materials such as photonic crystals [40], metamaterial [41], metasurface [42], and plasmonics [43] have been introduced, developed and utilized into THz regime. As low-dimension micro-nano structured media, metamaterial and metasurface offer unprecedented flexibility in the design and control of light propagation, which have been a research focus these years. They also show the capability on easily coupling with the THz Laser, imaging and communication systems. Isolator is a nonreciprocal one-way transmission device, which has an important application on the source protection, impedance matching, noise-cancelling and decoupling in the communication or radar system. However, lacking in feasible broadband low-loss one-way transmission devices in the THz regime such as isolator and circulator, THz echoes of the reflection and scattering between system components bring some noise, which limits the performance of these THz systems. However, the methods of ferrite isolators in microwave frequency and Faraday isolators at infrared regime both are inappropriate for THz frequencies, how to promote efficiency of

magneto-optical (MO) devices on nonreciprocal transmission at THz regime becomes a problem. It means that the one-way THz transmission principles still need to be investigated more deeply.

In this paper, we introduce our recent research on novel isolators and nonreciprocal transmission devices in THz regime. Based on MO microstructure, such as magnetic photonic crystal, magneto-plasmonics and magneto-metasurface, we realized one-way transmission through different forms of isolators. Moreover, we have analyzed and concluded the necessary conditions of forming THz nonreciprocal transmission in magneto-microstructure devices. It strongly depends on the magneto-material and asymmetric transmission system, which breaks the time reversal symmetry. Our basic and theoretic work on THz Isolators is important for high efficient THz systems.

2. Terahertz magneto-optical material

When the external magnetic field is along the x axis, the semiconductor InSb has a strong gyrotropy at the cyclotron frequency ω_c , while the ω_c can be expressed as $\omega_c=eB/m^*$, in which B is the magnetic flux density, showing the relation with the external magnetic field, m^* is the effective mass of the carrier and $m^*=0.015m_e$ for the InSb, m_e is the mass of electron; e is the electron charge. The dielectric function of InSb can be expressed as a nonreciprocal tensor under this configuration [33]:

$$\begin{bmatrix} \varepsilon_x & 0 & 0 \\ 0 & \varepsilon_y & -\varepsilon_{yz} \\ 0 & \varepsilon_{yz} & \varepsilon_z \end{bmatrix} \quad (1)$$

Three different tensor elements in Eq. (1) can be written as:

$$\begin{aligned} \varepsilon_x &= \varepsilon_\infty - \varepsilon_\infty \frac{\omega_p^2}{\omega(\omega + \gamma i)}, \\ \varepsilon_y &= \varepsilon_z = \varepsilon_\infty - \varepsilon_\infty \frac{\omega_p^2(\omega + \gamma i)}{\omega[(\omega + \gamma i)^2 - \omega_c^2]}, \\ \varepsilon_{yz} &= \varepsilon_\infty \frac{i\omega_p^2\omega_c}{\omega[(\omega + \gamma i)^2 - \omega_c^2]}, \end{aligned} \quad (2)$$

ε_∞ is the high-frequency limit permittivity, $\varepsilon_\infty=15.68$; ω is the angular frequency of the incident EM waves; γ is the collision frequency of carriers, $\gamma =e/(\mu m^*)=0.1 \pi \text{ THz}$; ω_p is plasma frequency written as $\omega_p=(Ne^2/\varepsilon_0 m^*)^{1/2}$, ε_0 is the free-space permittivity, and N is intrinsic carrier density which can be written as [35]:

$$N(\text{cm}^{-3}) = 5.76 \times 10^{14} T^{1.5} \exp[-0.26 / (2 \times 8.625 \times 10^{-5} \times T)]. \quad (3)$$

In fact, many works proves its good performance in the temperature 180 K~250 K. Therefore, the InSb material has the strong dispersion and gyrotropy in THz regime which can be controlled by the external magnetic field and temperature. It can deduced that $\text{Re}(\epsilon_y) = -\text{Im}(\epsilon_{yz})$ and $\text{Re}(\epsilon_{yz}) = \text{Im}(\epsilon_y)$, where Re represents the real part and Im represents imaginary part. The calculation on dielectric tensor elements in Fig.1 shows that the external magnetic field and temperature has a significant influence on the permittivity and strong dispersion.

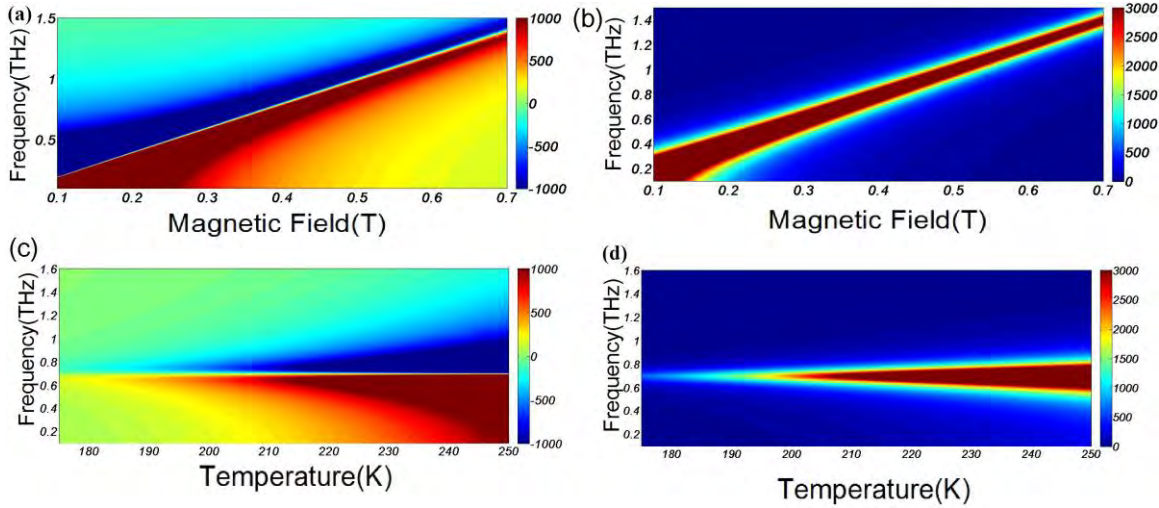


Fig. 1 Dielectric properties of the InSb with different external magnetic field and temperature. (a) ϵ_y and (b) ϵ_{yz} with the dependence of the external magnetic field at $T=230\text{ K}$; (c) ϵ_y and (d) ϵ_{yz} with the dependence of the temperature at $B=0.3\text{ T}$.

3. Magneto photonic crystal based on ferrofluid

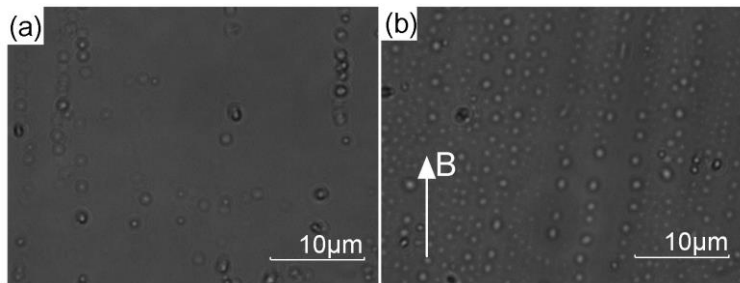


Fig. 2 Microscope images of ferrofluid (a) without and (b) with an EMF.

The combination between artificial electromagnetic materials and MO material may enhance the MO effect in the device. For example, in the optical regime, both an enhanced Voigt MO effect [44] and a giant enhancement of Faraday rotation[45] in a garnet-metal grating were demonstrated, respectively. The ferrofluid used in this work is Fe_3O_4 nanoparticles dispersed in

a light mineral oil carrier. As shown in Fig. 2, when the ferrofluid is not magnetized, the particles are randomly distributed and the fluid can be regarded as an isotropic material. A weak EMF can trigger the particles to form magnetic chain clusters along the EMF direction which exhibits a MO property, and the number of the cluster increases with the EMF increasing to saturated magnetization. The experiment results show that the refractive index and absorption coefficient of ferrofluid for THz waves increase with the nanoparticle concentration increasing in the ferrofluid. Moreover, two different THz MO effects have been found with different EMF, of which mechanisms have been theoretically explained well by microscopic structure induced refractive index change in the magnetization process and the transverse magneto-optical effect after the saturation magnetization [46]. This work suggests that ferrofluid is a promising MO material in the THz regime. Therefore, filling the ferrofluid into an artificial electromagnetic materials structure may enhance the MO response in the THz regime. Here, We have investigated THz MO properties of a ferrofluid and a ferrofluid-filled photonic crystal (FFPC) 错误!未找到引用源。 by using the THz-TDS.

We have applied the EMF as the Voigt configuration as shown in Fig. 3(a), and the THz transmission spectra of the FFPC are shown in Fig. 3(b). As the EMF increases, the original resonance dip gradually splits into two resonances. Their resonance frequencies gradually move to lower and higher frequencies compared to the original resonance, respectively, and their resonance intensities gradually increase with the EMF increasing. In this process, the transmittance at 1.04 THz gradually rises up from 1.1% at 0 mT to 40% at 150 mT, which experiences a transition from a resonance dip to a transmission peak. Therefore, this FFPC realizes a magnetically induced THz wave transparency at the central frequency of 1.04 THz with 150 GHz bandwidth. This periodically MO-dielectric hybrid model leads the MP mode splitting, and the finite element method simulation confirms the existence of the CW and CCW rotating MP modes as shown in Fig. 3(c). This THz microstructure MO device and its tunability scheme will have great potential applications in THz filtering, modulation and sensing.

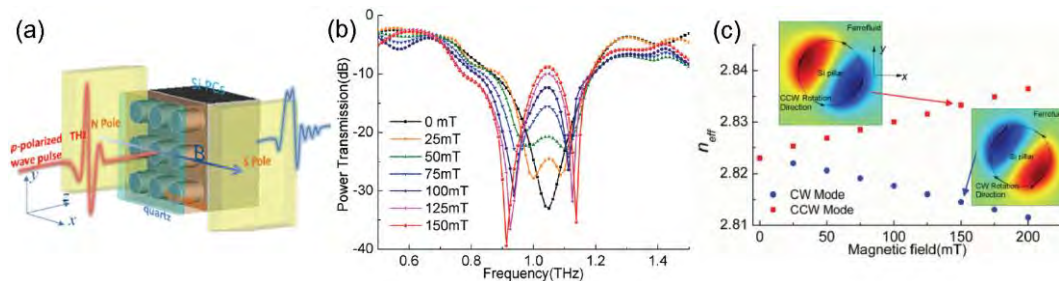


Fig. 3 (a) Schematic diagram of FFPC; (b) The experiment transmission spectra of the FFPC under the different EMF; (c) The dependence of the effective refractive indexes of the CCW and CW MP modes at 150 mT. [47]

4. Silicon-ferrite PC cavity circulator

Circulator is a kind of nonreciprocal devices [48], as shown in Fig.4(a). In this research we choose ferrite as the MO material. Ferrite is a kind of promising material for THz waves because of its small absorption loss and the existence of the ferromagnetic resonance. We take ferrite into photonic crystal forming a silicon-ferrite PCs circulator in the sub-THz region. By structure optimization and analysis of defect mode coupling, a tunable circulator is designed, of which central operating frequency can be tuned from 180 GHz to 205 GHz and the maximum isolation is 65.2 dB as shown in Fig. 4(d). The defected rotating dipole mode and the field patterns at operating frequency are shown in the Figs. 4(b) and 4(c). In our analysis, the PC cavity affects the mode confinement and spatial overlap of the magnetic material domain and defect modes; while the gyrotropy and ferromagnetic loss of the ferrite, induced and affected by magnetic field and THz frequency, have a great influence on the transmission and isolation property of this device. This circulator can realize the controllable splitting, filtering and isolating for THz applications.

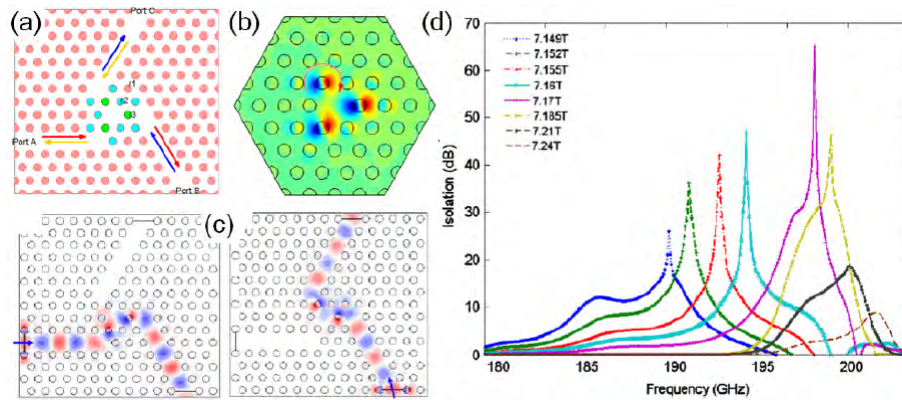


Fig. 4 Silicon-ferrite PC for THz circulator. (a) Schematic diagram; (b) Electric field pattern of defected rotating dipole mode; (c) Electric field patterns of the circulator; (d) isolation spectra under the different EMF.

5. Metal/Magneto-optical plasmonic waveguide

We propose a tunable THz isolator based on a metal/magneto-optical plasmonic waveguide (MMOPW) 错误!未找到引用源。 as shown in Fig. 5(a). Due to the introduction of periodic structure, the MMOPW shows a unique photonic band-gap characteristic that greatly enhances the one-way transmission, and obtains a lower insertion loss and higher isolation. Based on the dispersion and gyrotropy property of the InSb, the non-symmetrical photonic band-gap and one-way transmission property of the MMOPW are investigated in the THz regime. Due to the nonreciprocity of the InSb under the MF and the non-symmetry boundary conditions, the time reversal symmetry of the waveguide is broken, so the dispersion curves in the positive and negative propagation direction are different 错误!未找到引用源。 错误!未找到引用源。 Fig. 5(b) shows the dispersion relation of the MMOPW at $T=195\text{ K}$ with $B=1\text{ T}$. The dispersion curves show a significant photonic band structure due to the periodic structure of the SMPW. For the forward wave, a passband with high transmittances locates in 1.16-1.28 THz, and the maximum

transmittance is 95%. For the backward wave, no backward waves can propagate through the MMOPW in this frequency bands. As can be seen from the isolation spectra in Fig. 5(c), the device obtains its 30 dB isolation spectral width of larger than 80 GHz, the maximum isolation of higher than 90 dB at 1.18 THz, and the corresponding insertion loss of less than 5%. The further discussions show that the operating frequency band of this MMOPW isolator can be controlled by magnetic and thermal means.

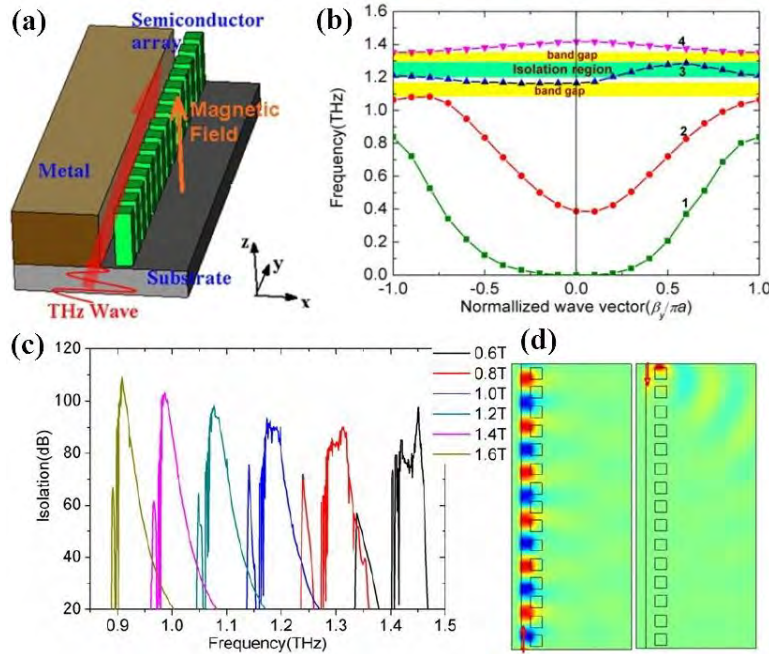


Fig. 5 (a) Schematic structure of the proposed MMOPW. (b) Band structure of the MMOPW when $T=195\text{ K}$, $B=1\text{ T}$. (c) Isolation spectra of the SMPW under the different EMF at $T=195\text{ K}$. (d) Electric field distributions of the SMPW when $T=195\text{ K}$ and $B=1\text{ T}$ of 1.2 THz forward wave and backward wave

6. Metal/magneto-optic plasmonic lens

Using surface plasmonic polaritons, the plasmonic lens can focus light beyond diffraction limit. The different phase retardations can be achieved by structuring the plasmonic lens to manipulate the spatial distribution of the output beam. Based on this, we proposed a THz isolator composed by a slit array with a periodic arrangement of the metal and InSb grating in turn [31] as shown in Fig. 6(a) called metal/magneto-optic plasmonic lens (MMOPL). Due to the MO material and asymmetric periodic structure, forward wave is focused while backward wave is reflected, forming nonreciprocal transmission. Compared with the previous single waveguide isolators, our MMOPL structure is an area array, chip-like device, which is much easier coupled in the space transmission system. Since our structure is larger than the area of THz beam, the THz beam does not have to be coupled by any waveguides. Therefore, the MMOPL has a smaller insertion loss.

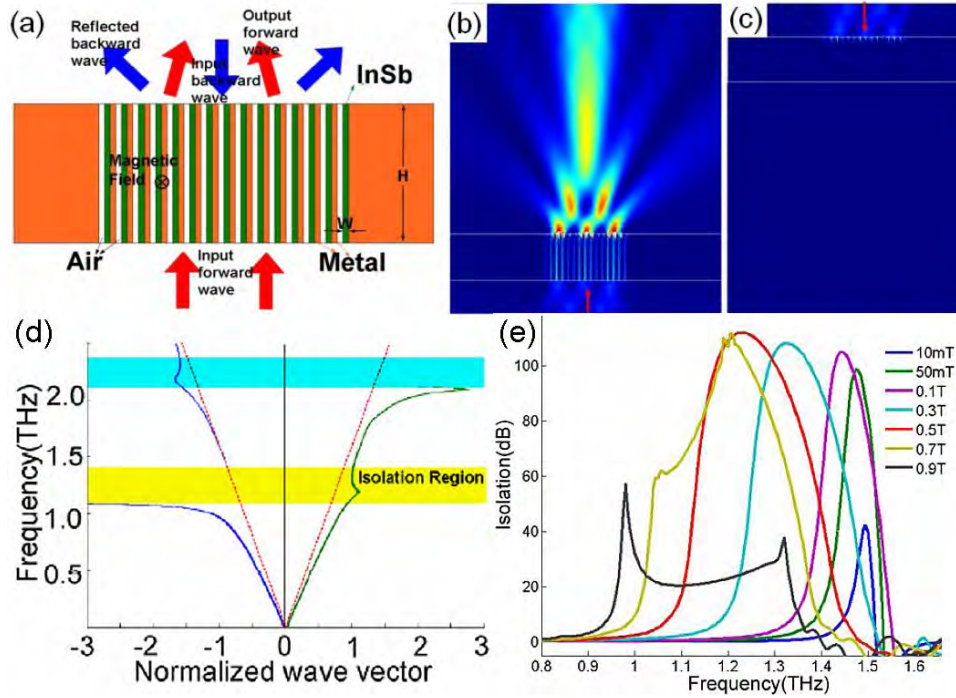


Fig. 6 (a) Schematic structure of the proposed MMOPL. (b) Forward and (c) backward power flow distributions through the MMOPL at 1.25 THz . (d) Dispersion relations of MMOPL at 185 K and 0.5 T . (e) Isolation spectra of the MMOPL under the different MF at 185 K

The asymmetrical dispersion relations of the proposed MMOPL are investigated in the THz regime as shown in Fig. 6(d). When there is no EMF applied, the dispersion curve is symmetric for the forward and backward propagation. When an EMF is applied as shown in Fig. 6(d), due to the gyrotropy of the InSb under the EMF and the non-symmetry structure, the SPPs split as two different MSPPs. Thus the dispersion curve becomes non-symmetric, the branch of the forward propagation moves to a higher frequency, and the backward moves to a lower frequency. For the backward wave, its bandgap is located at $1.45\text{-}1.55 \text{ THz}$ (yellow region in Fig. 6(d)), while the forward wave can still transmit at this frequency range. Therefore, this is an isolation region which permits the forward wave but forbids the backward wave. The numerical results show that the proposed isolator has an isolation bandwidth of larger than 0.4 THz and the maximum isolation of higher than 110 dB at the temperature of 185 K as shown in Fig. 6(e). The operating frequency of this device also can be broadly tuned by changing the external magnetic field or temperature. The further discussions show that a transmission enhancement through this MMOPL is about 30 times larger than that of the ordinary PLs. This low-loss, high isolation, broadband tunable nonreciprocal THz transmission mechanism has a great potential application in promoting the performances of the THz application systems.

7. Magneto-metasurface

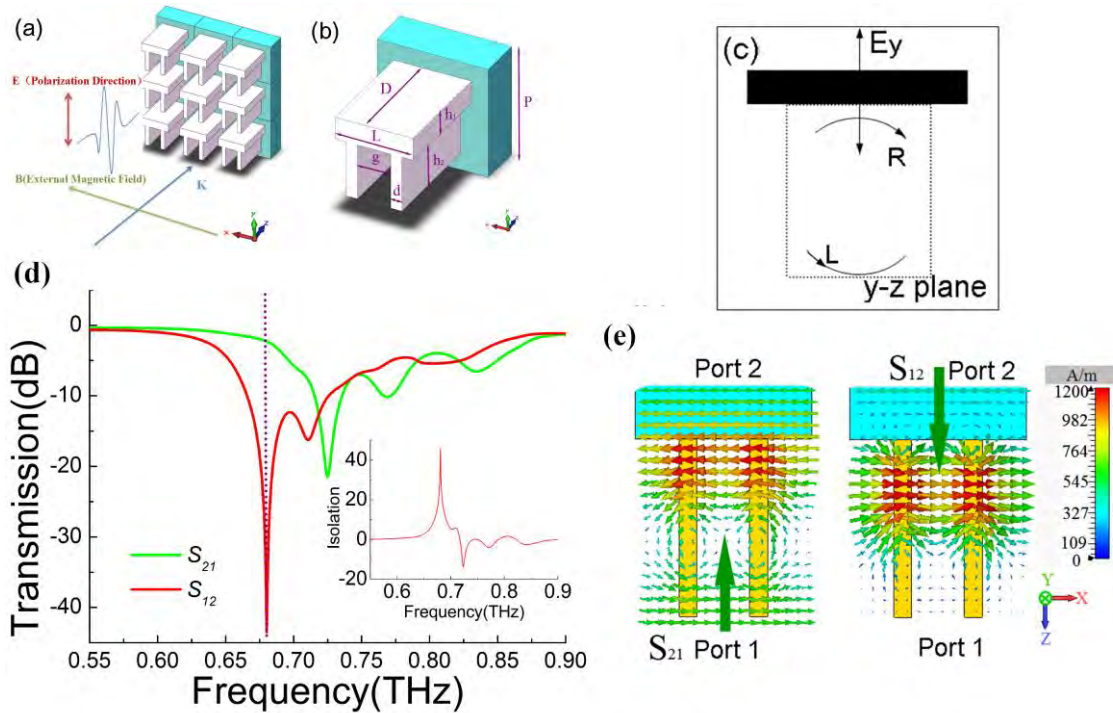


Fig. 7 (a) The 3D view of the device including the directions of the wave polarization and external magnetic field and the coordinate system in this work; (b) The geometry of the unit cell structure, $D = 50 \mu\text{m}$, $L=70 \mu\text{m}$, $P=100 \mu\text{m}$, $h_1=21 \mu\text{m}$, $g=30 \mu\text{m}$ and $h_2=50 \mu\text{m}$. (c) Asymmetric structure make the effective refractive indexes of the left and right rotating magneto-plasmon modes become different (d) The transmission spectrum of the forward waves $|S_{21}|^2$ and backward waves $|S_{12}|^2$, when $T=195 \text{ K}$, $B= 0.3 \text{ T}$, the inset picture is the isolation spectra of the isolator. (e) Steady magnetic field of the isolator at 0.68 THz when $T=195 \text{ K}$, $B= 0.3 \text{ T}$ in the x - z cut plane.

For easy coupling with the spatial THz waves, we have proposed a kind of magneto-metasurface [35], as shown in Fig.7, the resonance of forward and backward wave happen at not same frequency. When the backward wave has resonance at 0.678 THz , the forward wave at the same frequency band can transmit through this device. The reason that the resonance of forward and backward wave happen at different frequency is related with the MO structure. In fact, the resonance is induced by metasurface. If there is no MO material or if the MO material structure is symmetric along the y axis which is as same as the polarization direction, the resonance of forward and backward waves would happen at same frequency. However, in this Magneto-metasurface, the unit cell structure is asymmetric along the polarization direction of incident wave which indicates that the forward and backward waves are not equivalent and the effective refractive indexes of the left and right rotating magneto-plasmonic modes become different and split, as shown in Fig.7(c). It is why that the resonance of the forward and backward waves happens in different frequencies. This kind of the nonreciprocal resonance in the asymmetry magneto-metasurface can lead to a high isolation in the THz transmission system.

8. Conclusion

In conclusion, we have reviewed our study on THz isolators and nonreciprocal transmission devices: Metal/Magneto-optical plasmonic waveguide, plasmonic lens, silicon-ferrite PC cavity circulator and magneto-metasurface. Using the specific designed micro structure, the devices can realize the nonreciprocal transmission, which is different from the traditional isolators. The principles of our designing novel THz isolators above can be concluded as follows: (1) There should be MO material in the THz regime for the MO interaction between the incident waves and external magnetic field; (2) The transmission system needs be asymmetric for forward and backward waves in order to achieve the nonreciprocal transmission. For the MMOPW, the asymmetry transmission system is metal-air-InSb waveguide; for the MMOPL, it is metal-air-InSb grating; for Silicon-ferrite PC cavity circulator, it is asymmetric pillars in photonic crystal; for the magneto-metasurface, it is asymmetric structure for polarization of the transmitting waves. All of these form an asymmetric relation for forward and backward transmission. Besides, the oblique incidence can also break the asymmetry of the transmission system, but fail to break the time reversal symmetry. Our research work is new kind of attempt on novel THz isolators which is significant for the THz application system.

References

- [1] X.-C. Zhang, B. B. Hu, J. T. Darrow, et.al. "Generation of femtosecond electromagnetic pulses from semiconductor surfaces". *Appl. Phys. Lett.* 56, 1011 (1990).
- [2] J. Zhao, Y. Zhang, Z. Wang, et.al. "Propagation of terahertz wave inside femtosecond laser filament in air". *Laser Phys. Lett.* 11, 95302 (2014).
- [3] M. Shalaby and C. P. Hauri. "Spectrally intense terahertz source based on triangular Selenium". *Sci. Rep.* 5, 8059 (2015).
- [4] M. Rochat, L. Ajili, H. Willenberg, et.al. "Low-threshold terahertz quantum-cascade lasers". *Appl. Phys. Lett.* 81, 1381 (2002).
- [5] Y. Jiang, K. Vijayraghavan, S. Jung, et.al. "Broadly tunable external cavity terahertz source from 1.2~ 5.9 THz". in *Infrared, Millimeter, and Terahertz Waves (IRMMW-THz)*, 2014 39th International Conference on (IEEE, 2014), pp. 1–2.
- [6] T. Kleine-Ostmann and T. Nagatsuma. "A Review on Terahertz Communications Research". *J. Infrared, Millimeter, Terahertz Waves* 32, 143–171 (2011).
- [7] J. Zhao, W. Chu, L. Guo, et.al. "Terahertz imaging with sub-wavelength resolution by femtosecond laser filament in air". *Sci. Rep.* 4 (2014).
- [8] X. Wang, Z. Xie, W. Sun, et.al. "Focusing and imaging of a virtual all-optical tunable terahertz Fresnel zone plate.". *Opt. Lett.* 38, 4731–4 (2013).
- [9] K. B. Cooper, R. J. Dengler, G. Chattopadhyay et.al. "A High-Resolution Imaging Radar at 580 GHz". *IEEE*

- Microw. Wirel. Components Lett.* 18, 64–66 (2008).
- [10] E. S. Lee and T.-I. Jeon. "Tunable THz notch filter with a single groove inside parallel-plate waveguides." *Opt. Express* 20, 29605–12 (2012).
- [11] H.-T. Chen, W. J. Padilla, J. M. O. Zide et.al. "Ultrafast optical switching of terahertz metamaterials fabricated on ErAs/GaAs nanoisland superlattices". *Opt. Lett.* 32, 1620–1622 (2007).
- [12] J. Gu, R. Singh, X. Liu, et.al. "Active control of electromagnetically induced transparency analogue in terahertz metamaterials". *Nat. Commun.* 3, 1151 (2012).
- [13] Q. Y. Wen, H. W. Zhang, Q. H. Yang, et.al. "Terahertz metamaterials with VO₂ cut-wires for thermal tunability". *Appl. Phys. Lett.* 97, 23–26 (2010).
- [14] A. K. Azad, H.-T. Chen, S. R. Kasarla, et.al."Ultrafast optical control of terahertz surface plasmons in subwavelength hole arrays at room temperature". *Appl. Phys. Lett.* 95, 11105 (2009).
- [15] F. Fan, S. Chen, W.-H. Gu, et.al. "Active terahertz plasmonic crystal waveguide based on double-structured Schottky grating arrays". *Appl. Phys. Lett.* 105, 151110 (2014).
- [16] M. Rahm, J. S. Li, and W. J. Padilla. "THz wave modulators: A brief review on different modulation techniques". *J. Infrared, Millimeter, Terahertz Waves* 34, 1–27 (2013).
- [17] Z. Xie, X. Wang, J. Ye, et.al. "Spatial Terahertz Modulator". *Sci. Rep.* 3, 1–4 (2013).
- [18] T. He, B. Zhang, J. Shen, et.al. "High-efficiency THz modulator based on phthalocyanine-compound organic films". *Appl. Phys. Lett.* 106, 053303 (2015).
- [19] H.-T. Chen, W. J. Padilla, M. J. Cich et.al."A metamaterial solid-state terahertz phase modulator". *Nat. Photonics* 3, 148–151 (2009).
- [20] Y. Wu, C. La-o-vorakiat, X. Qiu, et.al. "Graphene Terahertz Modulators by Ionic Liquid Gating". *Adv. Mater.* (2015).
- [21] Q. Li, Z. Tian, X. Zhang, et.al."Active graphene–silicon hybrid diode for terahertz waves". *Nat. Commun.* 6, 7082 (2015).
- [22] T. J. Cui, M. Q. Qi, X. Wan, et.al. "Coding Metamaterials, Digital Metamaterials and Programming Metamaterials". *Light Sci. Appl.* 19 (2014).
- [23] Y. Zhang, S. Qiao, S. Liang, et.al."Gbps Terahertz External Modulator Based on a Composite Metamaterial with a Double-Channel Heterostructure". *Nano Lett.* 150429124146004 (2015).
- [24] F. Fan, Z. Guo, J.-J. Bai, et.al. "Magnetic photonic crystals for terahertz tunable filter and multifunctional polarization controller". *JOSA B* 28, 697–702 (2011).
- [25] B. Zhang, Q. Wu, C. Pan, et.al. "THz band-stop filter using metamaterials surfaced on LiNbO₃ sub-wavelength slab waveguide". *Opt. Express* 23, 16042 (2015).
- [26] X. Zhou, X. Yin, T. Zhang, et.al. "Ultrabroad terahertz bandpass filter by hyperbolic metamaterial waveguide". *Opt. Express* 23, 11657 (2015).
- [27] L. Cong, W. Cao, X. Zhang, et.al. "A perfect metamaterial polarization rotator". *Appl. Phys. Lett.* 103, 171107

(2013).

- [28] X. Wen and J. Zheng. "Broadband THz reflective polarization rotator by multiple plasmon resonances". *Opt. Express* 22, 28292–28300 (2014).
- [29] R.-H. Fan, Y. Zhou, X.-P. Ren, et.al. "Freely Tunable Broadband Polarization Rotator for Terahertz Waves". *Adv. Mater.* 27, 1201–1206 (2015).
- [30] S. C. Jiang, X. Xiong, Y. S. Hu, et.al. "Controlling the polarization state of light with a dispersion-free metastructure". *Phys. Rev. X* 4, 1–6 (2014).
- [31] F. Fan, S. Chen, X.-H. Wang, et.al. "Tunable nonreciprocal terahertz transmission and enhancement based on metal/magneto-optic plasmonic lens.". *Opt. Express* 21, 8614–8621 (2013).
- [32] Z. Xie, J. He, X. Wang, et.al. "Generation of terahertz vector beams with a concentric ring metal grating and photo-generated carriers". *Opt. Lett.* 40, 359–362 (2015).
- [33] F. Fan, S. J. Chang, W. H. Gu, et.al. "Magnetically tunable terahertz isolator based on structured semiconductor magneto plasmonics". *IEEE Photonics Technol. Lett.* 24, 2080–2083 (2012).
- [34] Y. Zhou, X. Xu, H. Fan, et.al. "Tunable magnetoplasmons for efficient terahertz modulator and isolator by gated monolayer graphene.". *Phys. Chem. Chem. Phys.* 15, 5084–5090 (2013).
- [35] S. Chen, F. Fan, X. Wang, et.al. "Terahertz isolator based on nonreciprocal magneto-metasurface". *Opt. Express* 23, 8614–8621 (2015).
- [36] M. Shalaby, M. Peccianti, Y. Ozturk, et.al. "A magnetic non-reciprocal isolator for broadband terahertz operation.". *Nat. Commun.* 4, 1558 (2013).
- [37] B. Hu, Q. J. Wang, and Y. Zhang. "Broadly tunable one-way terahertz plasmonic waveguide based on nonreciprocal surface magneto plasmons.". *Opt. Lett.* 37, 1895–7 (2012).
- [38] B. Hu, Q. J. Wang, and Y. Zhang. "A one-way terahertz plasmonic waveguide based on surface magneto plasmons in a metal-dielectric-semiconductor structure". *Proc. - Winter Simul. Conf.* 2, 357–359 (2013).
- [39] Y. Zhou, Y.-Q. Dong, K. Zhang, et.al. "Non-reciprocal transmission of terahertz waves through a photonic crystal cavity with graphene". *EPL (Europhysics Lett.)* 107, 54001 (2014).
- [40] I. A. Sukhoivanov and I. V Guryev. *Photonic Crystals: Physics and Practical Modeling* (Springer, 2009), Vol. 152.
- [41] T. J. Cui, D. R. Smith, and R. P. Liu. *Metamaterials* (Springer, 2010).
- [42] Y. Zhao, X.-X. Liu, and A. Alù. "Recent advances on optical metasurfaces". *J. Opt.* 16, 123001 (2014).
- [43] W. L. Barnes, A. Dereux, and T. W. Ebbesen. "Surface plasmon subwavelength optics.". *Nature* 424, 824–830 (2003).
- [44] V. I. Belotelov, I. A. Akimov, M. Pohl, et.al. "Enhanced magneto-optical effects in magnetoplasmonic crystals". *Nature Nanotechnology* 6, 370-376 (2011).
- [45] J.Y. Chin, T. Steinle, T. Wehler, et.al. "Nonreciprocal plasmonics enables giant enhancement of thin-film Faraday rotation". *Nature Communications* 4, 1599 (2013).

- [46] S. Chen, F. Fan, S. Chang, et. al. "Tunable optical and magneto-optical properties of ferrofluid in the terahertz regime". *Opt. Express* 22, 6313-6321 (2014).
- [47] F. Fan, S. Chen, W. Lin, et. al. "Magnetically tunable terahertz magnetoplasmons in ferrofluid-filled photonic crystals". *Appl. Phys. Lett.* 103, 161115 (2013).
- [48] F. Fan, S.-J. Chang, C. Niu, et.al. "Magnetically tunable silicon-ferrite photonic crystals for terahertz circulator". *Opt. Commun.* 285, 3763–3769 (2012).